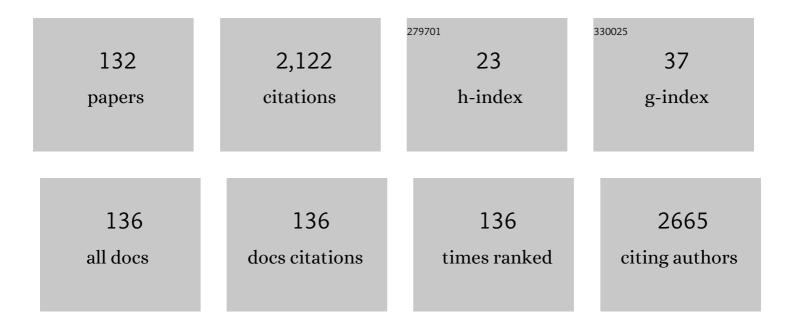
List of Publications by Year in descending order

Source: https://exaly.com/author-pdf/3162293/publications.pdf Version: 2024-02-01



#	Article	IF	CITATIONS
1	Microampere-level piezoelectric energy generation in Pb-free inorganic halide thin-film multilayers with Cu interlayers. Nano Energy, 2022, 92, 106785.	8.2	8
2	Room-temperature processed Ag/Pb(Zn1/3Nb2/3)O3–Pb(Zr0.5Ti0.5)O3-based composites for printable piezoelectric energy harvesters. Composites Science and Technology, 2022, 218, 109151.	3.8	5
3	Contribution of Anisotropic Latticeâ€6train to Piezoelectricity and Electromechanical Power Generation of Flexible Inorganic Halide Thin Films. Advanced Energy Materials, 2022, 12, .	10.2	14
4	Origin of the anisotropic-strain-driven photoresponse enhancement in inorganic halide-based self-powered flexible photodetectors. Materials Horizons, 2022, 9, 1207-1215.	6.4	11
5	Effect of transparent polymer encapsulation overlayers on bending fracture behavior of flexible organic lead halide perovskite thin films. Journal of Alloys and Compounds, 2022, 908, 164607.	2.8	2
6	Nanoampereâ€Level Piezoelectric Energy Harvesting Performance of Lithographyâ€Free Centimeterâ€Scale MoS ₂ Monolayer Film Generators. Small, 2022, 18, e2200184.	5.2	4
7	Origin of high piezoelectricity in carbon nanotube/halide nanocrystal/P(VDF-TrFE) composite nanofibers designed for bending-energy harvesters and pressure sensors. Nano Energy, 2022, 99, 107421.	8.2	19
8	Mechanical and piezoelectric properties of surface modified (Na,K)NbO3-based nanoparticle-embedded piezoelectric polymer composite nanofibers for flexible piezoelectric nanogenerators. Nano Energy, 2021, 79, 105445.	8.2	21
9	Anisotropic In Situ Strainâ€Engineered Halide Perovskites for High Mechanical Flexibility. Advanced Functional Materials, 2021, 31, 2007131.	7.8	22
10	Anisotropic in-situ stretching-strain engineering of flexible multilayer thin-film nanogenerators with Cu interlayers. Nano Energy, 2021, 82, 105690.	8.2	17
11	Origin of enhanced piezoelectric energy harvesting in all-polymer-based core–shell nanofibers with controlled shell-thickness. Composites Part B: Engineering, 2021, 223, 109141.	5.9	22
12	Graphitic carbon-based core-shell platinum electrocatalysts processed using nickel nanoparticle template for oxygen reduction reaction. Applied Surface Science, 2020, 533, 147519.	3.1	3
13	Large-Scale Self-Limiting Synthesis of Monolayer MoS ₂ via Proximity Evaporation from Mo Films. Crystal Growth and Design, 2020, 20, 2698-2705.	1.4	11
14	Radio frequency thermal plasma-processed Ni-W nanostructures for printable microcircuit electrodes. Materials and Design, 2020, 191, 108590.	3.3	2
15	Origin of high piezoelectricity of inorganic halide perovskite thin films and their electromechanical energy-harvesting and physiological current-sensing characteristics. Energy and Environmental Science, 2020, 13, 2077-2086.	15.6	54
16	<i>In situ</i> processed tungsten carbide/carbon black-supported platinum electrocatalysts for enhanced electrochemical stability and activity. Green Chemistry, 2020, 22, 2028-2035.	4.6	9
17	Enhanced dielectric properties and grain boundary potentials in sulfur-doped CaCu3Ti4O12 thin films. Journal of the European Ceramic Society, 2020, 40, 2375-2381.	2.8	7
18	In-situ stretching strain-driven high piezoelectricity and enhanced electromechanical energy-harvesting performance of a ZnO nanorod-array structure. Nano Energy, 2020, 72, 104735.	8.2	38

#	Article	IF	CITATIONS
19	Balanced Performance Enhancements of aâ€InGaZnO Thin Film Transistors by Using Allâ€Amorphous Dielectric Multilayers Sandwiching Highâ€k CaCu 3 Ti 4 O 12. Advanced Electronic Materials, 2019, 5, 1900322.	2.6	5
20	Stretching-Driven Crystal Anisotropy and Optical Modulations of Flexible Wide Band Gap Inorganic Thin Films. ACS Applied Materials & Interfaces, 2019, 11, 41516-41522.	4.0	2
21	Na-Mediated Stoichiometry Control of FeS2 Thin Films: Suppression of Nanoscale S-Deficiency and Improvement of Photoresponse. ACS Applied Materials & Interfaces, 2019, 11, 43244-43251.	4.0	9
22	Study on Lil and KI with low melting temperature for electrolyte replenishment in molten carbonate fuel cells. International Journal of Hydrogen Energy, 2019, 44, 25930-25938.	3.8	9
23	Enhanced CO Oxidation and Cyclic Activities in Three-Dimensional Platinum/Indium Tin Oxide/Carbon Black Electrocatalysts Processed by Cathodic Arc Deposition. ACS Applied Materials & Interfaces, 2019, 11, 25179-25185.	4.0	11
24	A review on binary metal sulfide heterojunction solar cells. Solar Energy Materials and Solar Cells, 2019, 200, 109963.	3.0	82
25	Flexible piezoelectric energy generators based on P(VDF-TrFE) nanofibers. Materials Research Express, 2019, 6, 086311.	0.8	13
26	Effective two-step chemical deposition for homogeneous lead sulfide thin films on a flexible polymer substrate. Thin Solid Films, 2019, 679, 1-7.	0.8	4
27	Electric-Field-Dependent Surface Potentials and Vibrational Energy-Harvesting Characteristics of Bi(Na _{0.5} Ti _{0.5})O ₃ -Based Pb-Free Piezoelectric Thin Films. ACS Applied Materials & Interfaces, 2019, 11, 13244-13250.	4.0	15
28	Nanoindentation and Bending Fracture Behavior of Flexible Sulfide Thin Films Grown at Near Room Temperature With in Situ Tensile/Compressive Stress. Advanced Engineering Materials, 2019, 21, 1801329.	1.6	3
29	Giant dielectric constant and tunable phaseâ€transition characteristics of ZnF 2 /BaF 2 â€modified BaTiO 3 thick films. International Journal of Applied Ceramic Technology, 2019, 16, 862-867.	1.1	0
30	Internal-field-dependent low-frequency piezoelectric energy harvesting characteristics of in situ processed Nb-doped Pb(Zr,Ti)O3 thin-film cantilevers. Journal of Alloys and Compounds, 2019, 781, 898-903.	2.8	5
31	Plasmonic-Enhanced Luminescence Characteristics of Microscale Phosphor Layers on a ZnO Nanorod-Arrayed Glass Substrate. ACS Applied Materials & Interfaces, 2019, 11, 1004-1012.	4.0	14
32	Direct Correlations of Grain Boundary Potentials to Chemical States and Dielectric Properties of Doped CaCu ₃ Ti ₄ O ₁₂ Thin Films. ACS Applied Materials & Interfaces, 2018, 10, 16203-16209.	4.0	23
33	Densification behavior and electrical properties of carbon nanotube-Ni nanocomposite films for co-fireable microcircuit electrodes. Thin Solid Films, 2018, 660, 754-758.	0.8	4
34	Flexible micro-scale UV-curable phosphor layers screen-printed on a polymer substrate for planar white light-emitting diodes. Materials Letters, 2018, 217, 124-126.	1.3	7
35	Quantitative analysis of improved bending fracture behavior of large-scale graphene monolayer-intervened flexible oxide thin films. Journal of Materials Chemistry C, 2018, 6, 6125-6131.	2.7	10
36	Quantitative analysis of bending fracture resistance of nanoscale Cu-buffered ZnO:Al thin films on a polymer substrate. Journal of Alloys and Compounds, 2018, 731, 49-54.	2.8	9

#	Article	IF	CITATIONS
37	Structural, optical and electrical impacts of marcasite in pyrite thin films. Solar Energy, 2018, 159, 930-939.	2.9	22
38	Experimental Demonstration of in Situ Stress-Driven Optical Modulations in Flexible Semiconducting Thin Films with Enhanced Photodetecting Capability. Chemistry of Materials, 2018, 30, 7776-7781.	3.2	12
39	Origin of Prestress-Driven Optical Modulations of Flexible ZnO Thin Films Processed in Stretching Mode. Journal of Physical Chemistry Letters, 2018, 9, 5934-5939.	2.1	11
40	Piezoelectric energy harvesting and charging performance of Pb(Zn1/3Nb2/3)O3–Pb(Zr0.5Ti0.5)O3 nanoparticle-embedded P(VDF-TrFE) nanofiber composite sheets. Composites Science and Technology, 2018, 168, 296-302.	3.8	29
41	Large Localâ€Compressive Stressâ€Induced Improvements in Piezoelectric Characteristics of Lead Zirconate Titanate Thin Films on a Ni Nanodots Array. Advanced Electronic Materials, 2018, 4, 1800081.	2.6	1
42	In Situ Synthesis of Bimetallic Tungsten-Copper Nanoparticles via Reactive Radio-Frequency (RF) Thermal Plasma. Nanoscale Research Letters, 2018, 13, 220.	3.1	16
43	Simple prismatic patterning approach for nearly room-temperature processed planar remote phosphor layers for enhanced white luminescence efficiency. Optical Materials Express, 2018, 8, 3230.	1.6	3
44	Origin of in Situ Domain Formation of Heavily Nb-Doped Pb(Zr,Ti)O ₃ Thin Films Sputtered on lr/TiW/SiO ₂ /Si Substrates for Mobile Sensor Applications. ACS Applied Materials & Interfaces, 2017, 9, 18904-18910.	4.0	25
45	High-Efficiency Double Absorber PbS/CdS Heterojunction Solar Cells by Enhanced Charge Collection Using a ZnO Nanorod Array. ACS Omega, 2017, 2, 4894-4899.	1.6	23
46	Origin of Abnormal Dielectric Behavior and Chemical States in Amorphous CaCu ₃ Ti ₄ O ₁₂ Thin Films on a Flexible Polymer Substrate. Chemistry of Materials, 2017, 29, 5915-5921.	3.2	17
47	Enhanced piezoelectric and imprint characteristics of in situ sputtered Ta-doped Pb(Zr,Ti)O 3 thin films on Ir/TiW/SiO 2 /Si substrates. Journal of Alloys and Compounds, 2017, 720, 369-375.	2.8	9
48	Controlled post-sulfurization process for higher efficiency nontoxic solution-deposited CuIn0.7Ga0.3Se2 absorber thin films with graded bandgaps. Journal of Alloys and Compounds, 2017, 710, 177-181.	2.8	4
49	Dielectric and current–voltage characteristics of flexible Ag/BaTiO ₃ nanocomposite films processed at near room temperature. RSC Advances, 2017, 7, 56038-56043.	1.7	5
50	Micro-scale roughening of glass substrates using carbon nanotube-driven templates for enhancements in white luminescence characteristics. Optics Letters, 2017, 42, 5094.	1.7	3
51	Improved Photovoltaic Characteristics and Grain Boundary Potentials of Culn _{0.7} Ga _{0.3} Se ₂ Thin Films Spin-Coated by Na-Dissolved Nontoxic Precursor Solution. ACS Applied Materials & Interfaces, 2016, 8, 17011-17015.	4.0	18
52	Dielectric Characteristics of <scp>UV</scp> urable CaCu ₃ Ti ₄ O ₁₂ Composite Thick Film Capacitors on Cu Foils. International Journal of Applied Ceramic Technology, 2016, 13, 685-689.	1.1	4
53	Enhanced Luminescence Characteristics of Remote Yellow Silicate Phosphors Printed on Nanoscale Surface-Roughened Class Substrates for White Light-Emitting Diodes. Advanced Optical Materials, 2016, 4, 1081-1087.	3.6	24
54	Insertion of Vertically Aligned Nanowires into Living Cells by Inkjet Printing of Cells. Small, 2016, 12, 1446-1457.	5.2	12

#	Article	IF	CITATIONS
55	Origin of the enhanced electrical characteristics of BaTiO3-based thermistors by sputtered Al and Ni–Cu buffer electrode films. Current Applied Physics, 2016, 16, 435-439.	1.1	2
56	Whiteâ€Lightâ€Emitting Diodes: Enhanced Luminescence Characteristics of Remote Yellow Silicate Phosphors Printed on Nanoscale Surfaceâ€Roughened Glass Substrates for White Lightâ€Emitting Diodes (Advanced Optical Materials 7/2016). Advanced Optical Materials, 2016, 4, 976-976.	3.6	4
57	Effect of double substitutions of Cd and Cu on optical band gap and electrical properties of non-colloidal PbS thin films. Journal of Alloys and Compounds, 2016, 685, 129-134.	2.8	16
58	Enhanced optical and piezoelectric characteristics of transparent Ni-doped BiFeO ₃ thin films on a glass substrate. RSC Advances, 2016, 6, 16602-16607.	1.7	29
59	Optical and grain boundary potential characteristics of sulfurized BiFeO3 thin films for photovoltaic applications. Dalton Transactions, 2016, 45, 5598-5603.	1.6	5
60	White luminescence characteristics of red/green silicate phosphor-glass thick film layers printed on glass substrate. Optical Materials Express, 2016, 6, 938.	1.6	13
61	Piezoelectric Energy Harvesting Characteristics of GaN Nanowires Prepared by a Magnetic Field-Assisted CVD Process. Journal of the Korean Ceramic Society, 2016, 53, 167-170.	1.1	8
62	Effect of band-aligned double absorber layers on photovoltaic characteristics of chemical bath deposited PbS/CdS thin film solar cells. Scientific Reports, 2015, 5, 14353.	1.6	22
63	Highly efficient flexible CuIn0.7Ga0.3Se2 solar cells with a thick Na/Mo layer deposited directly on stainless steel. Applied Surface Science, 2015, 346, 562-566.	3.1	14
64	(Na,K)NbO3 nanoparticle-embedded piezoelectric nanofiber composites for flexible nanogenerators. Composites Science and Technology, 2015, 111, 1-8.	3.8	104
65	Improved photovoltaic and grain boundary characteristics of single elementary target-sputtered Cu ₂ ZnSnSe ₄ thin films by post sulfurization/selenization process. Journal Physics D: Applied Physics, 2015, 48, 245103.	1.3	6
66	Tensile Stress-Dependent Fracture Behavior and Its Influences on Photovoltaic Characteristics in Flexible PbS/CdS Thin-Film Solar Cells. ACS Applied Materials & amp; Interfaces, 2015, 7, 4573-4578.	4.0	20
67	Enhanced Fracture Resistance of Flexible ZnO:Al Thin Films in Situ Sputtered on Bent Polymer Substrates. ACS Applied Materials & Interfaces, 2015, 7, 17569-17572.	4.0	35
68	Prestress Driven Improvement in Fracture Behavior of in Situ Sputtered Zinc Oxide Thin Films on Stretched Polymer Substrates. ACS Applied Materials & Interfaces, 2015, 7, 14654-14659.	4.0	10
69	Long-Term Stable, Low-Temperature Remote Silicate Phosphor Thick Films Printed on a Glass Substrate. ACS Combinatorial Science, 2015, 17, 234-238.	3.8	31
70	Doped SnO ₂ Transparent Conductive Multilayer Thin Films Explored by Continuous Composition Spread. ACS Combinatorial Science, 2015, 17, 247-252.	3.8	17
71	UV-curable silicate phosphor planar films printed on glass substrate for white light-emitting diodes. Optics Letters, 2015, 40, 3723.	1.7	17
72	Single elementary target-sputtered Cu2ZnSnSe4 thin film solar cells. Solar Energy Materials and Solar Cells, 2015, 132, 136-141.	3.0	36

#	Article	IF	CITATIONS
73	Origin of the enhanced photovoltaic characteristics of PbS thin film solar cells processed at near room temperature. Journal of Materials Chemistry A, 2014, 2, 20112-20117.	5.2	80
74	Silicon Carbide Whiskerâ€Reinforced Ceramic Tape for Highâ€Power Components. International Journal of Applied Ceramic Technology, 2014, 11, 240-245.	1.1	4
75	RF power dependence of refractive index of room temperature sputtered ZnO:Al thin films. Applied Physics A: Materials Science and Processing, 2014, 115, 347-351.	1.1	4
76	Fabrication of surface-textured ZnO:Al/ITO bilayers with enhanced electrical and light-scattering properties. Solid State Sciences, 2014, 31, 75-80.	1.5	5
77	In Situ Magnetic Field-Assisted Low Temperature Atmospheric Growth of GaN Nanowires via the Vapor–Liquid–Solid Mechanism. ACS Applied Materials & Interfaces, 2014, 6, 116-121.	4.0	11
78	Iron pyrite thin films deposited via non-vacuum direct coating of iron-salt/ethanol-based precursor solutions. Journal of Materials Chemistry A, 2014, 2, 17779-17786.	5.2	24
79	High Quality Mn-Doped (Na,K)NbO ₃ Nanofibers for Flexible Piezoelectric Nanogenerators. ACS Applied Materials & Interfaces, 2014, 6, 10576-10582.	4.0	142
80	Spatial and RF power dependence of the structural and electrical characteristics of copper zinc tin selenide thin films prepared by single elementary target sputtering. Materials Chemistry and Physics, 2014, 148, 175-180.	2.0	2
81	Full Range Dielectric Characteristics of Calcium Copper Titanate Thin Films Prepared by Continuous Composition-Spread Sputtering. ACS Combinatorial Science, 2014, 16, 478-484.	3.8	15
82	Enhanced dielectric and tunable characteristics of K-doped Ba0.5Sr0.5TiO3 thin films prepared by pulsed laser deposition. Thin Solid Films, 2013, 527, 267-272.	0.8	18
83	Unusual near-band-edge photoluminescence at room temperature in heavily-doped ZnO:Al thin films prepared by pulsed laser deposition. Materials Chemistry and Physics, 2013, 140, 610-615.	2.0	2
84	Preparation and visible-light photocatalysis of hollow rock-salt TiO1â^'xNx nanoparticles. Journal of Materials Chemistry A, 2013, 1, 3639.	5.2	19
85	Characteristics of Cu2ZnSnSe4 and Cu2ZnSn(Se,S)4 absorber thin films prepared by post selenization and sequential sulfurization of co-evaporated Cu–Zn–Sn precursors. Journal of Alloys and Compounds, 2013, 579, 279-283.	2.8	30
86	Densification, Crystallization, and Dielectric Properties of <scp><scp>AlN</scp></scp> , <scp>BN</scp> , and <scp><scp>Si</scp></scp> ₃ <scp><<scp>N</scp>4 Filler ontaining <scp>LTCC</scp> Materials. International Journal of Applied Ceramic Technology, 2013, 10, E25.</scp>	1.1	8
87	Surface scaling evolution and dielectric properties of sputter-deposited low loss Mg 2 SiO 4 thin films. Surface and Coatings Technology, 2013, 231, 229-233.	2.2	9
88	Sputter-deposited low loss Mg2SiO4 thin films for multilayer hybrids. Thin Solid Films, 2013, 527, 250-254.	0.8	3
89	Phase development, microstructure and optical properties of Cu 2 ZnSnSe 4 thin films modified with Pb and Ti. Surface and Coatings Technology, 2013, 231, 389-393.	2.2	6
90	Effective Laser Sealing Enabled by Glass Thick Films Containing Carbon Black/Carbon Nanotubes. Journal of the American Ceramic Society, 2013, 96, 1113-1117.	1.9	4

#	Article	IF	CITATIONS
91	Corrosion behavior of highly-crystallizable BaO–Nd2O3–TiO2–B2O3 glass-based composites. Corrosion Science, 2013, 66, 399-403.	3.0	5
92	Effects of SiO2 interlayer on electrical properties of Al-doped ZnO films under bending stress. Electronic Materials Letters, 2012, 8, 375-379.	1.0	10
93	Phase evolution and enhanced dielectric properties of BaO·Nd 2 O 3 ·TiO 2 ·B 2 O 3 glass-based dielectrics containing CaCu 3 Ti 4 O 12. Journal of Alloys and Compounds, 2012, 530, 40-47.	2.8	5
94	Barium Neodymium Titanium Borate Glassâ€Based High <i>k</i> Dielectrics. Journal of the American Ceramic Society, 2012, 95, 1356-1359.	1.9	6
95	Thickness-dependent tunable characteristics of (Ba0.5Sr0.5)0.925K0.075TiO3 thin films prepared by pulsed laser deposition. Current Applied Physics, 2012, 12, 654-658.	1.1	11
96	Chemically Driven Zero Shrinkage Dielectric Ceramics. Journal of the American Ceramic Society, 2012, 95, 1796-1798.	1.9	5
97	Structural and Raman Scattering Properties of ZnO:Al Thin Films Sputter-Deposited at Room Temperature. Journal of the Electrochemical Society, 2011, 159, H96-H101.	1.3	9
98	Thickness-dependent fracture behaviour of flexible ZnO : Al thin films. Journal Physics D: Applied Physics, 2011, 44, 025401.	1.3	39
99	Effect of Zn and Ca modifications on crystallization and microwave dielectric properties of lanthanum borates. Journal of Alloys and Compounds, 2011, 509, 849-853.	2.8	17
100	Phase evolution and grain-boundary contributions in CaCu3â^'xZnxTi4O12. Electronic Materials Letters, 2011, 7, 337-341.	1.0	7
101	Spatial Variation in Structural, Morphological and Optical Properties of Aluminum-Doped ZnO Thin Films Grown by 30°-Incident Radio Frequency Magnetron Sputtering. Journal of the Electrochemical Society, 2011, 158, P30.	1.3	12
102	Enhanced PTCR Characteristics of 0.95BaTiO[sub 3]–0.05(Bi[sub 0.5]Na[sub 0.5])TiO[sub 3] Ceramics Fabricated by Modified Synthesis Process. Journal of the Electrochemical Society, 2011, 158, J27.	1.3	7
103	Enhanced electrical properties of pulsed laser-deposited Culn0.7Ga0.3Se2 thin films via processing control. Solar Energy, 2010, 84, 2213-2218.	2.9	23
104	Crystallization and surface segregation in Culn0.7Ga0.3Se2 thin films on Cu foils grown by pulsed laser deposition. Applied Surface Science, 2010, 256, 6819-6823.	3.1	26
105	Enhanced Quality Factor of Zinc Lanthanum Borates-Based Dielectrics via the Control of ZnO/B2O3Ratio. Journal of the American Ceramic Society, 2010, 93, 334-337.	1.9	13
106	Bismuth Borosilicateâ€Based Thick Film Passivation of Ag Grid for Largeâ€Area Dye‣ensitized Solar Cells. Journal of the American Ceramic Society, 2010, 93, 1554-1556.	1.9	11
107	Dielectric and Grainâ€Boundary Characteristics of Hot Pressed CaCu ₃ Ti ₄ O ₁₂ . Journal of the American Ceramic Society, 2010, 93, 2419-2422.	1.9	30
108	Calcium Aluminoborosilicateâ€Based Dielectrics Containing CaCu ₃ Ti ₄ O ₁₂ as a Filler. Journal of the American Ceramic Society, 2010, 93, 2334-2338.	1.9	16

#	Article	IF	CITATIONS
109	Preparation and electrical properties of CuInSe ₂ thin films by pulsed laser deposition using excess Se targets. Journal of Materials Research, 2010, 25, 1936-1942.	1.2	2
110	AlN Passivation Layer-Mediated Improvement in Tensile Failure of Flexible ZnO:Al Thin Films. ACS Applied Materials & Interfaces, 2010, 2, 2471-2474.	4.0	21
111	Improved electrochemical properties of Li(Ni0.7Co0.3)O2 cathode for lithium ion batteries with controlled sintering conditions. Journal of Applied Electrochemistry, 2009, 39, 671-679.	1.5	6
112	Crystallization behavior and microwave dielectric characteristics of ZnO-(La, Nd)2O3-B2O3-based dielectrics. Journal of Electroceramics, 2009, 23, 127-132.	0.8	7
113	Effects of various oxide fillers on physical and dielectric properties of calcium aluminoborosilicate-based dielectrics. Journal of Electroceramics, 2009, 23, 185-190.	0.8	24
114	Phase evolution and Sn-substitution in LiMn2O4 thin films prepared by pulsed laser deposition. Journal of Electroceramics, 2009, 23, 200-205.	0.8	11
115	Physical and dielectric properties of BaTiO3–fluoride–glass systems for nitrogen-fireable embedded capacitors. Journal of Electroceramics, 2009, 23, 277-283.	0.8	2
116	Structural and Electrical Characteristics of ZnO Thin Films on Polycrystalline AlN Substrates. Journal of the American Ceramic Society, 2009, 92, 665-670.	1.9	5
117	Boron Nitride-Based Overcoat Thick Films for MoSi2Planar Heating Elements. Journal of the American Ceramic Society, 2009, 92, 1867-1870.	1.9	0
118	Shrinkage behavior of LTCC hetero-laminates. Journal of the European Ceramic Society, 2009, 29, 711-716.	2.8	17
119	Stress-induced anomalous shift of optical band gap in ZnO:Al thin films. Applied Physics Letters, 2009, 95, .	1.5	129
120	Chemical durability of anorthite-based low temperature co-fired ceramics. Journal of the Ceramic Society of Japan, 2009, 117, 1138-1140.	0.5	3
121	Gadolinium Zinc Borate Glass-Based Low Temperature Co-fired Ceramics. Metals and Materials International, 2008, 14, 493-496.	1.8	6
122	Refiring Performance of Calcium Aluminoborosilicate-Based Dielectrics. Journal of the American Ceramic Society, 2008, 91, 2727-2729.	1.9	3
123	Chemical stability and dielectric properties of RO–La2O3–B2O3 (R=Ca, Mg, Zn)-based ceramics. Materials Research Bulletin, 2008, 43, 361-369.	2.7	28
124	Improved cycleability of LiMn2O4-based thin films by Sn substitution. Applied Physics Letters, 2008, 93, .	1.5	6
125	Crystallization and dielectric properties of low temperature dielectrics containing Li2O filler. Journal of Non-Crystalline Solids, 2008, 354, 3849-3853.	1.5	5
126	Thick Film Capacitors with Variable Tc on Cu Foils. Materials Research Society Symposia Proceedings, 2008, 1075, 1.	0.1	0

#	Article	IF	CITATIONS
127	Influences of alkali oxides on crystallization and dielectric properties of anorthite-based low temperature dielectrics. Journal of the Ceramic Society of Japan, 2008, 116, 825-828.	0.5	10
128	Improvement of Temperature Coefficient of Frequency in Ba-deficient Ba5Nb4O15 Microwave Dielectrics. Journal of the Ceramic Society of Japan, 2007, 115, 978-981.	0.5	3
129	Influences of Particle Size of Alumina Filler in an LTCC System. Journal of the American Ceramic Society, 2007, 90, 649-652.	1.9	44
130	Low-Temperature High-k Dielectrics for Embedded Microcircuit Systems. Journal of the Korean Physical Society, 2007, 51, 181.	0.3	2
131	Phase Evolution and Microwave Dielectric Properties of Lanthanum Borate-Based Low-Temperature Co-Fired Ceramics Materials. Journal of the American Ceramic Society, 2006, 89, 060428035142031-???.	1.9	24
132	Dielectric properties of the BaTiO3-AlN-additive system. Journal of Electroceramics, 2006, 17, 461-465.	0.8	2